Spatial extent of $\Delta(1232)$ with $\pi^0\pi^0$ correlations with BGOegg

何庆华（HE Qinghua）

for LEPS2/BGOegg collaboration

Nanjing University of Aeronautics and Astronautics (NUAA), China

Aug. 10, 2022

Contents

- Motivation
- BEC measurements in the non-perturbative QCD energy region
- Event mixing method
- Correlation observation model
- Results of FOREST and BGOegg experiments
- Summary

Motivation

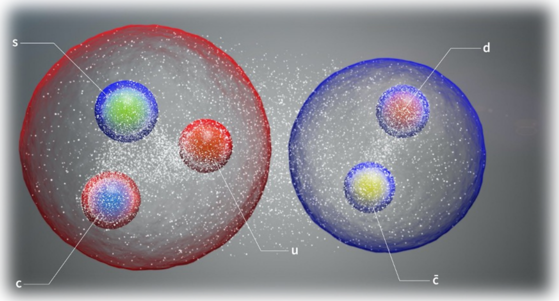

- Understanding the **strong interaction mechanism** in the **non-perturbative QCD energy region** is one of the main challenges in quark nuclear physics.

- Measuring the **properties of hadrons** in the non-perturbative QCD energy region is one of the powerful tools to understand the hadron structure and strong interaction.

- We experimentally measure unstable hadron **spatial dimensions** via photo-production in the baryon resonance region (BGOegg: 1.3-2.4 GeV; FOREST: 0.5-1.2 GeV) through identical meson **Bose-Einstein correlations**.

Motivation

BGOegg exp. : 1.3-2.4 GeV

FOREST exp. : 0.5-1.2 GeV

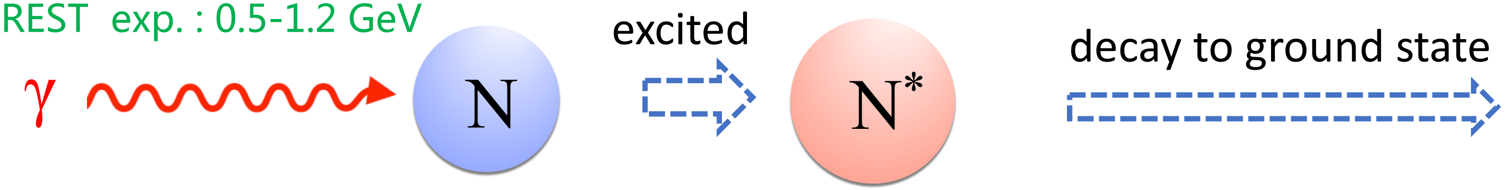

Correlation function:

$$g^{(2)}(p_1, p_2) = \frac{I_{12}(p_1, p_2)}{I_1(p_1)I_2(p_2)}$$

Assuming Gaussian density distribution of emitting source

$$g^{(2)}(Q) = N(1 + \lambda_2 e^{-r_0^2 Q^2})$$

source size of a multi-pion emitter

2 or more than 2 identical bosons

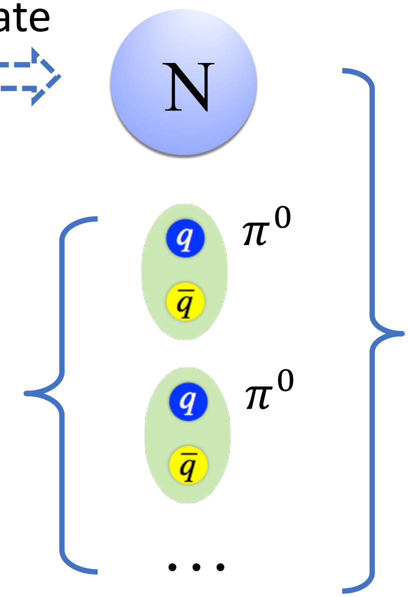

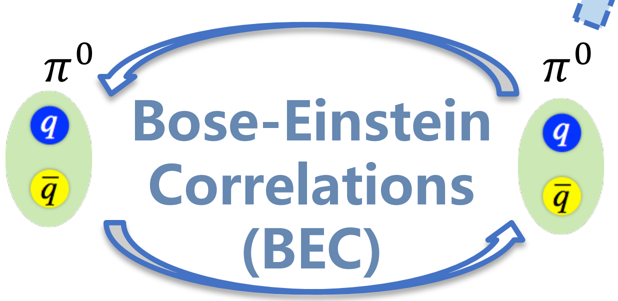

Bose-Einstein Correlations between identical particles provides a tool to measure the space-time properties of the boson emission source.

Motivation

Hanbury Brown-Twiss (HBT) Effects

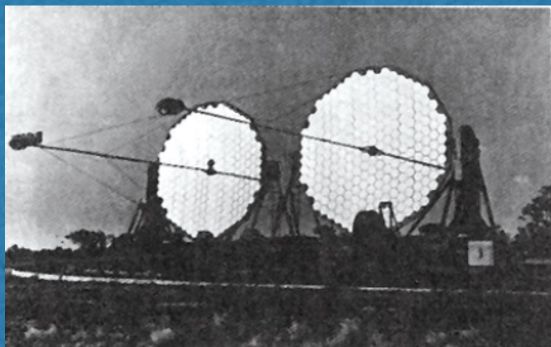

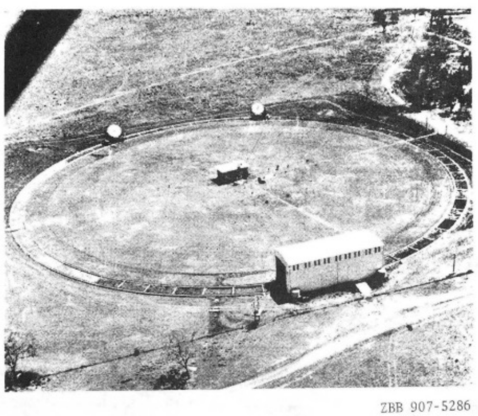

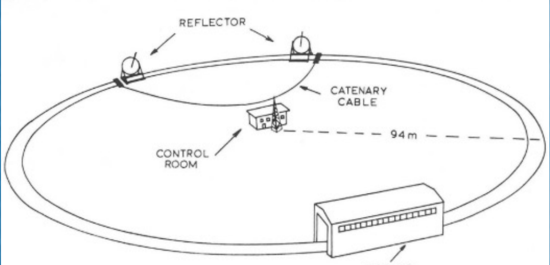

图片来源：G. Goldhaber, Proc. Int. Workshop on Correlations and Mul- tiparticle production (CAMP - LESIP IV), p. 409, ed. by M L Plümer, S Raha and R M Weiner, World Scientific (1991).

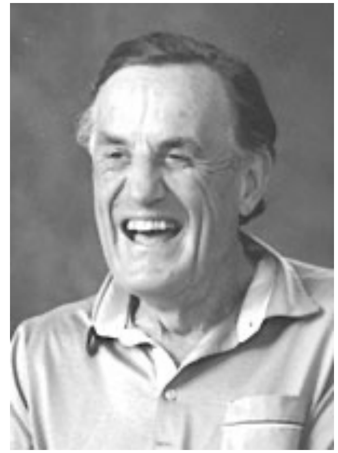

Robert Hanbury Brown
1916-2002

Richard Quentin Twiss
1920-2005

1956，Robert Hanbury Brown and Richard Q. Twiss introduced the intensity interferometer concept to radio astronomy for measuring the tiny angular size of f Sirius

Hanbury Brown- Twiss (HBT) effects

- **Bose–Einstein correlations (bosons)**
- **Fermi–Dirac correlations(fermions)**

Motivation

Hanbury Brown-Twiss (HBT) Effects

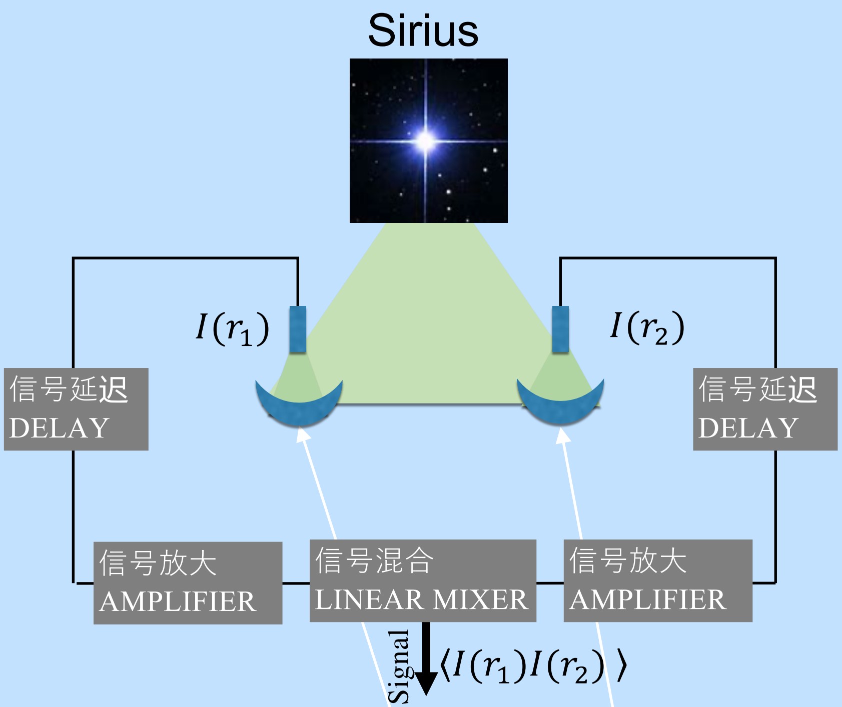

Average over coincidence measurements

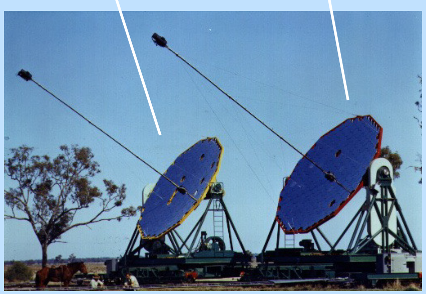

THE HANBURY BROWN-TWISS INTENSITY INTERFEROMETER AT NARRABRI, NEW SOUTH WALES, AUSTRALIA
Picture from： http://quantumtantra.com/quim.html

Sirius angular size:
0.0063”

Intensity interference：

$$g^{(2)}(r_1, r_2) = \frac{\langle I(r_1)I(r_2)\rangle}{\langle I(r_1)\rangle\langle I(r_2)\rangle}$$

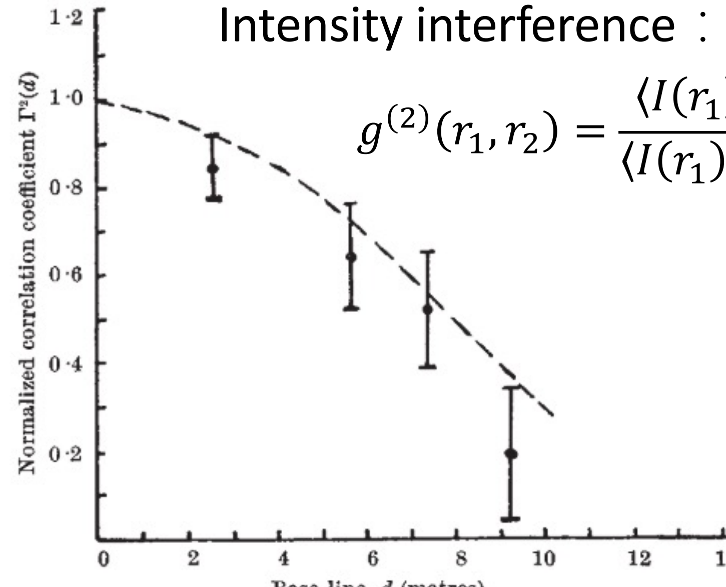

Fig. 2. Comparison between the values of the normalized correlation coefficient Γ²(d) observed from Sirius and the theoretical values for a star of angular diameter 0·0063″. The errors shown are the probable errors of the observations

图片来源：Hanbury Brown R 1956 A test of new type of new steller interferometer on SIRIUS *Nature* **178**

Motivation

Hanbury Brown-Twiss (HBT) Effects

1960s,HBT in particle physics

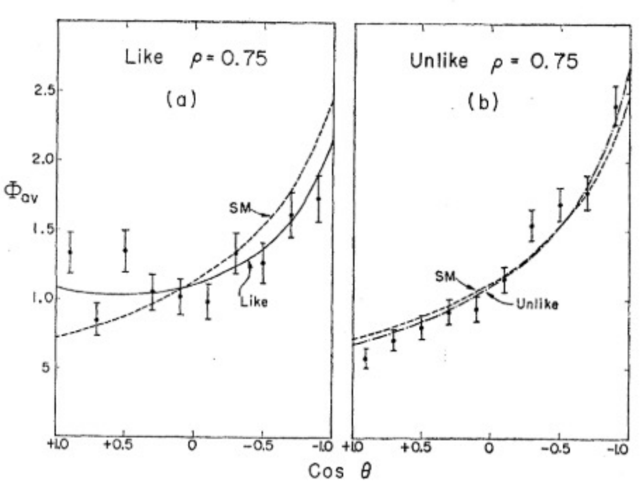

FIG. 6. The functions $\Phi_{av}(\cos\theta)$ computed at $\rho=0.75$ are compared with the experimental distribution of angles between pion pairs. Figures 6(a) and 6(b) give the distributions for like and unlike pions respectively. Also shown in each is the curve for $\Phi_{av}^{SM}(\cos\theta)$, the statistical distribution, without the effect of correlation functions. Here Φ_{av} represents an average of Φ_4, Φ_5, and Φ_6, weighted according to the individual charge channels. The experimental data comes from reference 1 (see also Table I, footnote a).

Ref：G. Goldhaber, S. Goldhaber, W. Lee, and A. P ais, Phys. Rev. **120**, 300 (1960).

Non-symmetrized two-particle wave function

$$\Psi^{s}{}_{0} = e^{i(k_1 r_1 + k_2 r_2)}$$

Symmetrized two-particle wave function

$$\Psi^{s}{}_{BE} = \frac{1}{\sqrt{2}}[e^{i(k_1 r_1 + k_2 r_2)} + e^{i(k_1 r_2 + k_2 r_1)}]$$

Bose-Einstein correlations (BEC) of two pions

Lawrence Radiation Laboratory and Department of Physics, University of California, Berkeley, California

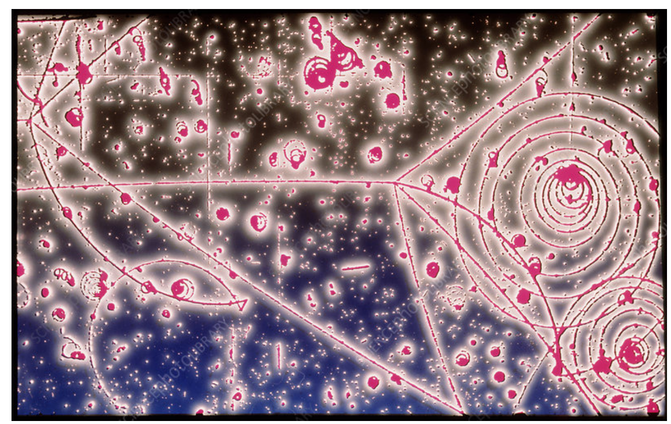

Annihilation in a bubble chamber. False-colour image from a hydrogen bubble chamber showing th e annihilation of an antiproton (horizontal line entering at left) and a proton. The annihilation even t has occurred at the intersection point just right of centre. Only charged particles leave tracks in s uch chambers; the passage of neutral particles has to be inferred from these data. Spiral tracks are due to low-energy electrons and positrons. In modern, extremely high- energy particle experiment s, the bubble chamber has been supplanted by electronic detectors.
图片来源： https://www.sciencephoto.com/media/1355/view

Motivation

Hanbury Brown-Twiss (HBT) Effects

HBT in heavy ion collisions

Table 1: The two-pion emitter dimension r_2 and the chaoticity parameter λ_2 obtained from Bose-Einstein Correlation (BEC) analysis for a variety of hadron reactions. The data marked with superscribe ^{a} indicats the choice for the reference sample is the $\pi^+\pi^-$ data sample, while ^{b} means the reference samples are either Monte Carlo generated events or a sample constructed by the event mixing technique.

$BE-System$	Reaction	Experiment	E_{cm}	$r_2(fm)$	λ_2
$\pi^\pm\pi^\pm$	$e^+e^-\to h$	MARK II [2]	29	0.75 ± 0.05^a	0.28 ± 0.04^a
				0.97 ± 0.11^b	0.27 ± 0.04^b
$\pi^\pm\pi^\pm$	$e^+e^-\to h$	TPC [3]	29	0.65 ± 0.06^b	0.50 ± 0.04^b
$\pi^\pm\pi^\pm$	$e^+e^-\to h$	TASSO [4]	34	0.82 ± 0.07^a	0.35 ± 0.03^a
$\pi^\pm\pi^\pm$	$e^+e^-\to h$	AMY [5]	58	0.73 ± 0.21^a	0.47 ± 0.07^a
				0.58 ± 0.06^b	0.39 ± 0.05^b
$\pi^\pm\pi^\pm$	$e^+e^-\to h$	ALEPH [6]	91	0.82 ± 0.04^a	0.48 ± 0.03^a
				0.52 ± 0.02^b	0.30 ± 0.01^b
$\pi^\pm\pi^\pm$	$e^+e^-\to h$	DELPHI [7]	91	0.83 ± 0.03^a	0.31 ± 0.02^a
				0.47 ± 0.03^b	0.24 ± 0.02^b
$\pi^\pm\pi^\pm$	$e^+e^-\to h$	L3 [8]	91	0.46 ± 0.02^b	0.29 ± 0.03^b
$\pi^\pm\pi^\pm$	$e^+e^-\to h$	OPAL [1]	91	0.96 ± 0.02^a	0.67 ± 0.03^a
				0.79 ± 0.02^b	0.58 ± 0.01^b
$\pi^\pm\pi^\pm$	$\gamma\gamma\to h$	[2]	5	1.05 ± 0.08	1.20 ± 0.13
$\pi^\pm\pi^\pm$	$\gamma\gamma\to 6\pi^\pm$	[11]	1.6-7.5	0.54 ± 0.22	0.59 ± 0.20
$\pi^\pm\pi^\pm$	$\nu(\bar{\nu})N\to h$	[12]	8-64	0.64 ± 0.16	0.46 ± 0.16
$\pi^\pm\pi^\pm$	$\mu p\to h$	[13]	23	0.65 ± 0.03	0.80 ± 0.07
$\pi^\pm\pi^\pm$	$\pi^+p\to h$	[14]	21.7	0.83 ± 0.06	0.33 ± 0.02
$\pi^\pm\pi^\pm$	$pp\to h$	[15]	26	1.02 ± 0.20	0.32 ± 0.08
$\pi^\pm\pi^\pm$	$pp\to h$	[16]	27.4	1.20 ± 0.03	0.44 ± 0.01
$\pi^\pm\pi^\pm$	$pp\to h$	[17]	63	0.82 ± 0.05	0.40 ± 0.03
$\pi^\pm\pi^\pm$	$\bar{p}p\to h$	[18]	1.88	1.04 ± 0.01	1.96 ± 0.03
$\pi^\pm\pi^\pm$	$\bar{p}p\to h$	[19]	200-900	0.73 ± 0.03	0.25 ± 0.02
$\pi^\pm\pi^\pm$	$ep\to eh$	[20]	$2.45<Q_\gamma<10$	0.68 ± 0.06	0.52 ± 0.20
$\pi^\pm\pi^\pm$	$ep\to eh$	[21]	$10.5<Q_\gamma$	0.67 ± 0.04	0.43 ± 0.09
$\pi^0\pi^0$	$e^+e^-\to h$	L3 [8, 9]	91	0.31 ± 0.10^b	0.16 ± 0.09^b
$\pi^0\pi^0$	$e^+e^-\to h$	OPAL [10]	91	0.59 ± 0.11^b	0.55 ± 0.15^b
$k^\pm k^\pm$	$ep\to eh$	[22]	$E_e:27.5;E_p:820$	$0.37\pm0.07^{+0.09}_{-0.08}$	$0.57\pm0.09^{+0.15}_{-0.08}$
$k^0_Sk^0_S$	$ep\to eh$	[22]	$E_e:27.5;E_p:820$	$0.70\pm0.19^{+0.28+0.38}_{-0.08-0.52}$	$0.63\pm0.09^{+0.07+0.09}_{-0.08-0.02}$

强度关联函数

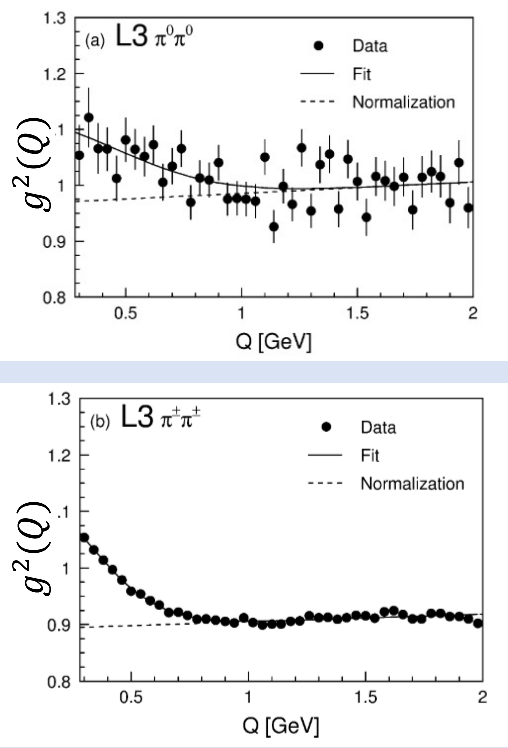

Fig. 4. Distribution of $g^2(Q)$ for (a) π0π0 a nd (b) π±π±, and results of the fits. The poi nts indicate the data, the full line correspon ds to the fit result and the dashed line is the normalization factor N(1 +αQ).

Ref: Achard P, et al 2002 Bose–Einstein correlations of neutral and charged pions in hadronic Z decays *Phys. Lett. B* **524** 55–64

BEC measurements in the non-perturbative QCD energy region

Photoproduction in the non-perturbative QCD energy region

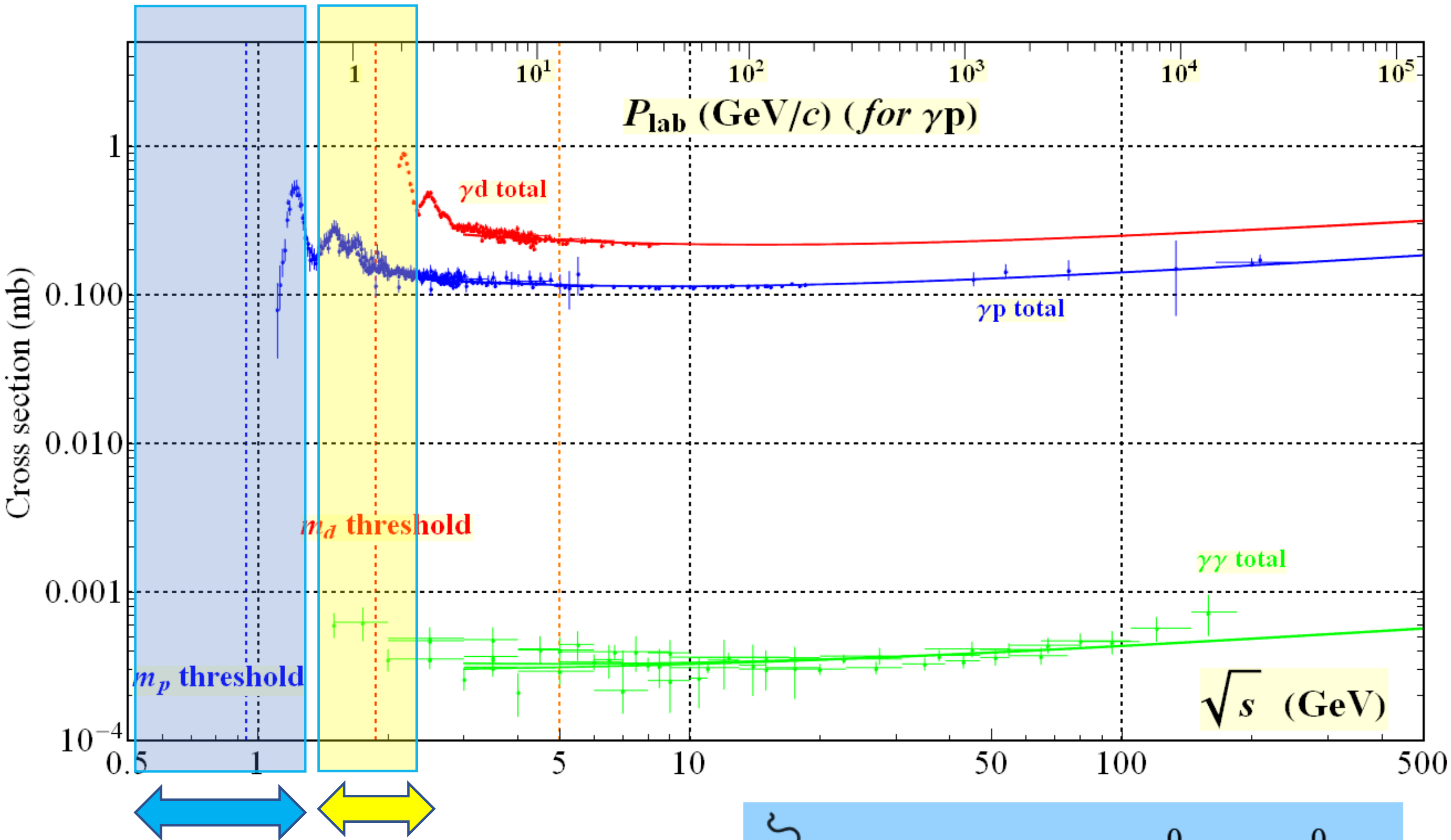

FOREST Exp.

BGOegg Exp.

0.5 GeV≤E_γ≤1.2 GeV

1.3 GeV≤E_γ≤2.4 GeV

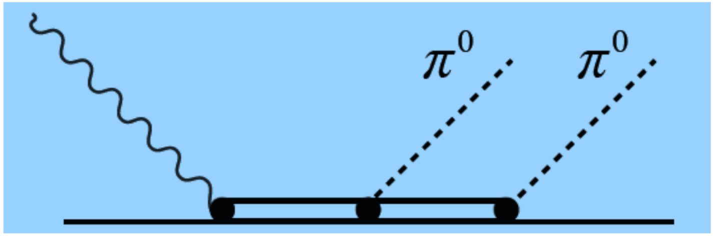

BEC measurements in the non-perturbative QCD energy region

(1) Event mixing method

low energies low multiplicities	high energies high multiplicities
strongly disturbed by non-BEC factors of exclusive reactions with a low multiplicity such as **global conservation laws** and decays of **resonances**	**weakly disturbed** by non-BEC factors such as **global conservation laws**
Complicated kinematical constraints	Simple kinematical constraints

(2) Resonance decay effects

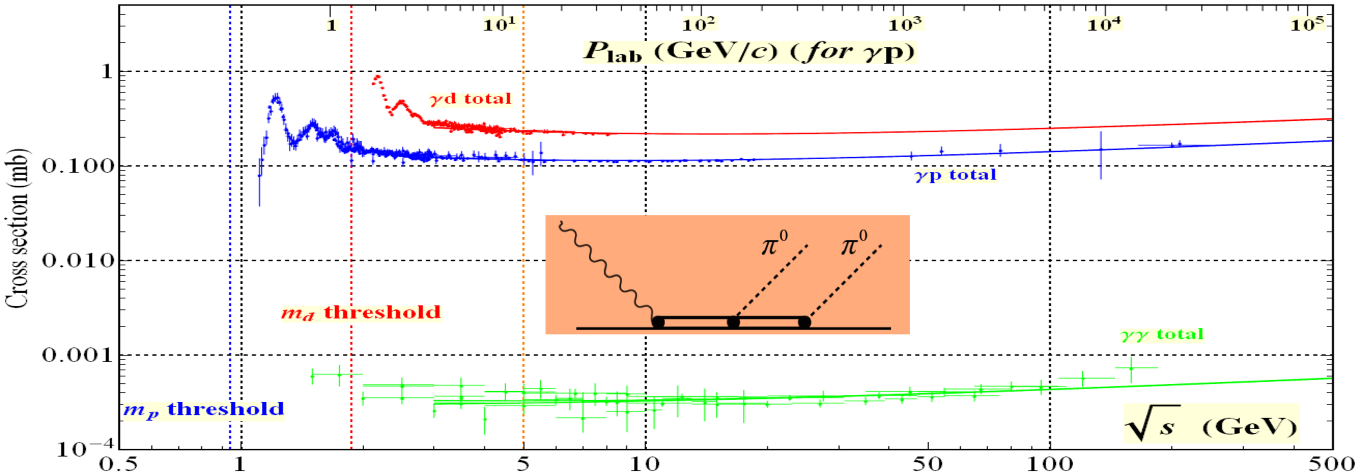

Event mixing method

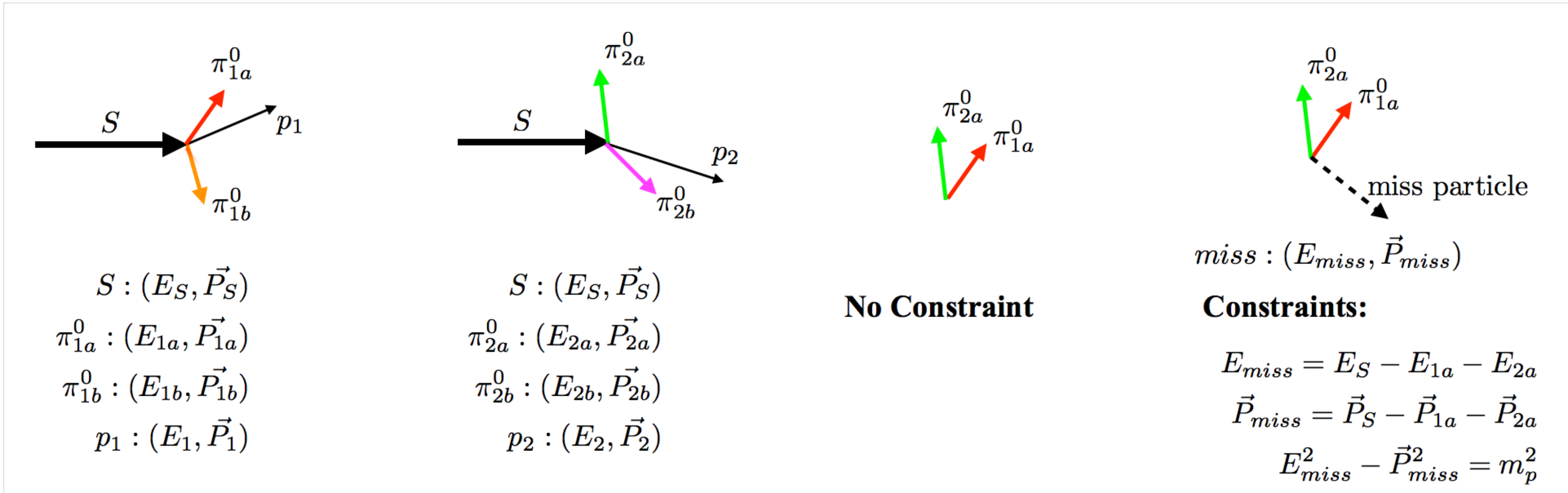

(a) Event 1 (b) Event 2 (c) Mixed Event (d) Mixed Event

Appropriate mixing cuts should be applied in the mixing

- **Missing mass consistency (MMC) cut :** $\left|m_X^{mix} - m_X^{ori}\right| < M_{cut}$
- **Pion energy (PE) cut:** events with pion energy higher than a given level are rejected
- **Energy sum order (ESO) cut:** $\mathbf{min}(E_{sum}^{ori,1}, E_{sum}^{ori,2}) < E_{sum}^{mix} < \mathbf{max}(E_{sum}^{ori,1}, E_{sum}^{ori,2})$
- **no overlapping photon clusters** (used to correct the detection efficiency)
- ……

Event mixing method

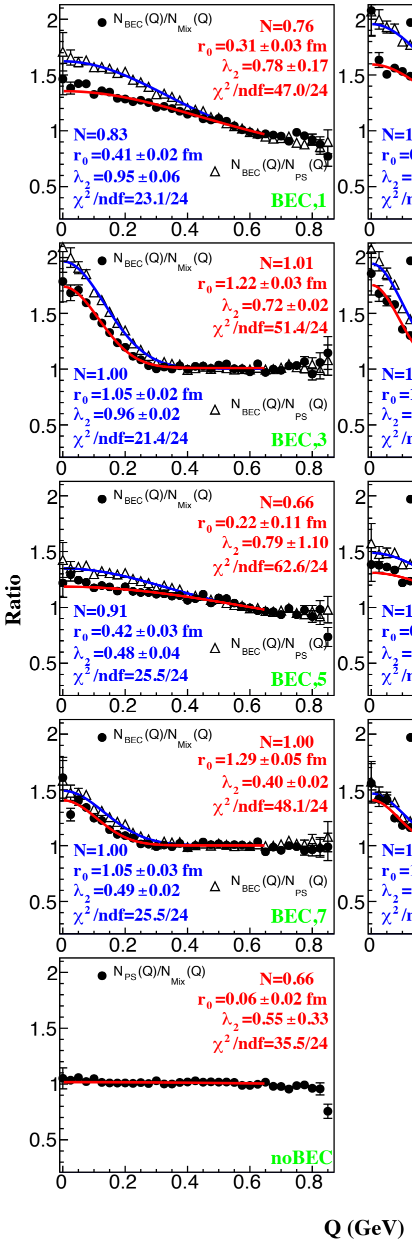

Appropriate mixing cuts in event mixing: MMC + PE cuts

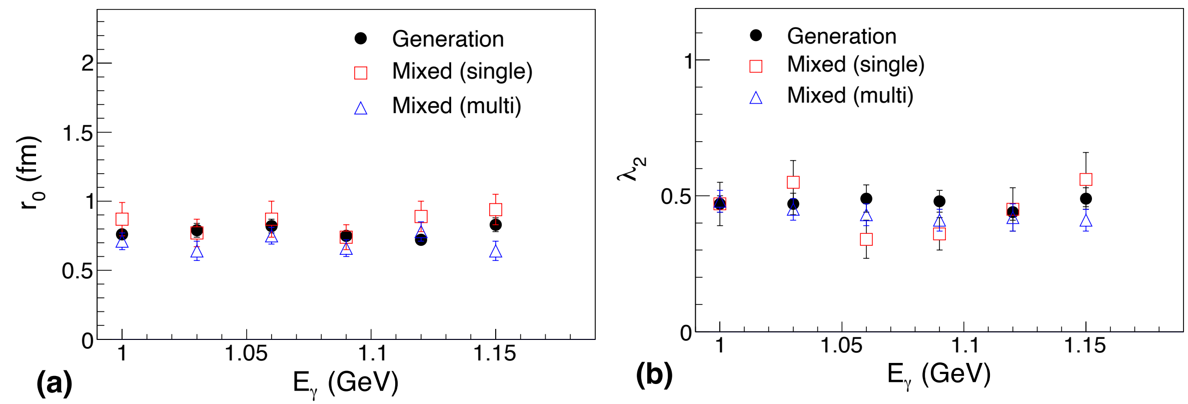

Fig. Fitted values of r_0 (a) and λ_2 (b) obtained by event mixing in a single-and a multi mixing (up to 10 times) mode at six incident photon energies E_γ=1.0, 1.03, 1.06, 1.09, 1.12, and 1.15 GeV for the $\gamma p \rightarrow \pi^0\pi^0 p$ events. For comparison, the values of r_0 and λ_2 for the generated sample with BEC effects are also shown.

Fig. The ratio of the Q distribution of the generated BEC/noBEC sample, $N_{BEC}(Q)$, to that from the mixed events, $N_{Mix}(Q)$ (filled circles). The ratio of $N_{BEC}(Q)$ to the Q distribution of pure phase space sample, $N_{PS}(Q)$, is also shown (open triangles) in each panel for comparison.

[1] Q. He, et al., Acta Phys. Pol. B **51**, 463 (2020); **[2]** Q. He, et al., Prog. Theor. Exp. Phys. **2017**, (2017);
[3] Q.-H. He, et al., Chinese Phys. C **40**, 114002 (2016).

Correlation observation model

- S wave meson emission due to an energetic quark

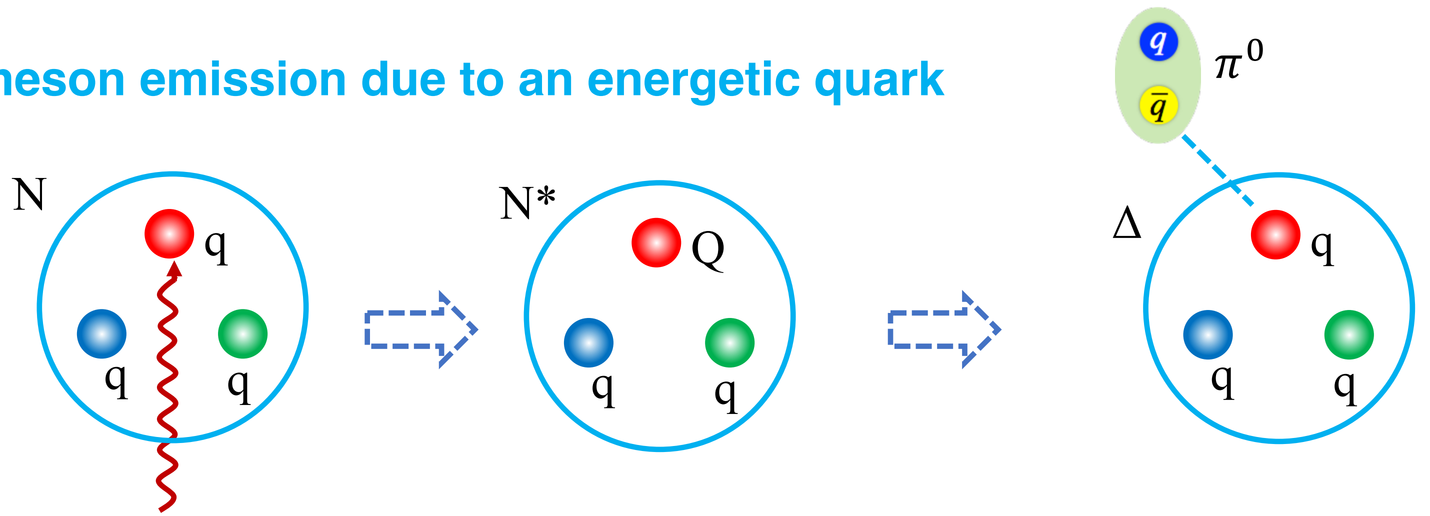

- Δ→π⁰N decay originated by an energetic quark Q

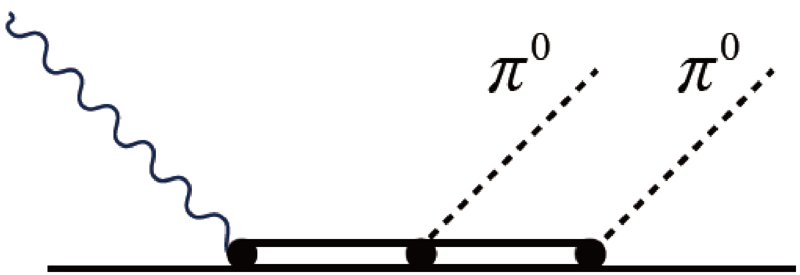

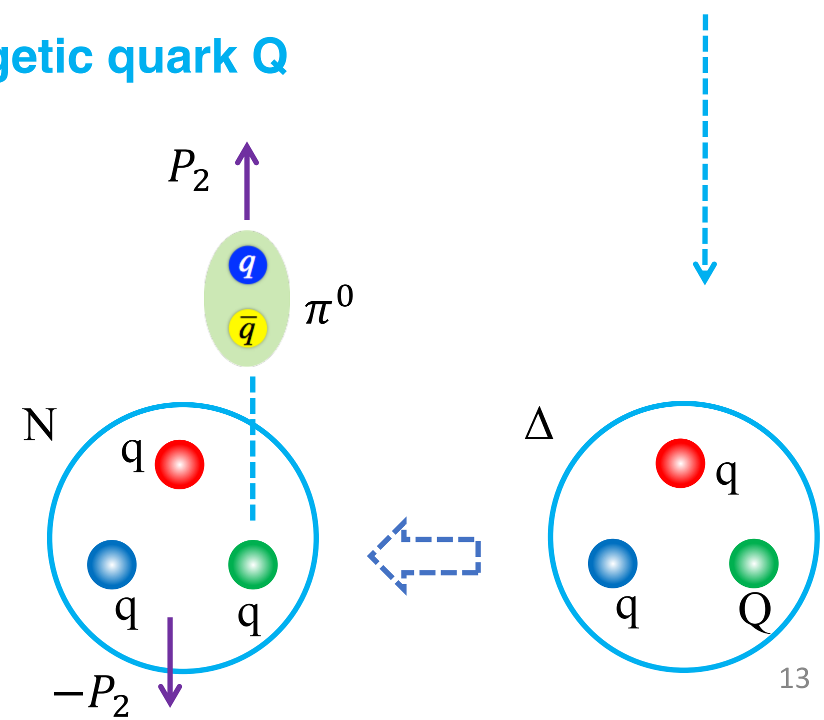

H. Shimizu, ELPH Annual Report, 2017

Correlation observation model

3-d correlation function

$$C_{BEC}(q,p_2) = 1 + \lambda \exp\left(-\frac{\alpha^2 q^2}{2}\right) \exp\left(-\frac{\alpha^2 q_z^2}{2}\right) J_0(\beta q_r)$$

$$= 1 + \lambda \exp(-\alpha^2 q_z^2) \exp\left(-\frac{\alpha^2 q_r^2}{2}\right) J_0(\beta q_r)$$

$\boldsymbol{\alpha}$: Gaussian radius

$\boldsymbol{\lambda}$: correlation strength

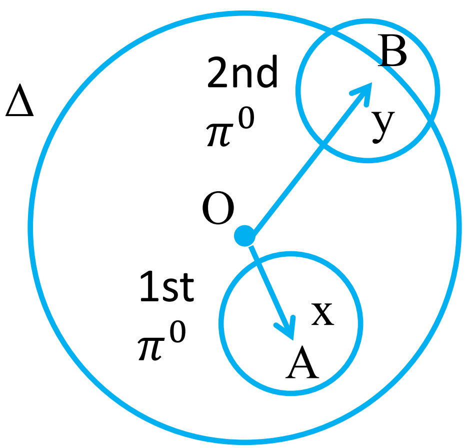

Space-time coordinates of Δ at rest

$\boldsymbol{q}$: relative momentum of two pions in the frame of Δ at rest

$\vec{q} = (q_r, 0, q_z)$ in cylindrical coordinates $\quad q^2 = q_r^2 + q_z^2$

$$\boldsymbol{\beta} = \frac{1}{2p_2}$$

$\boldsymbol{p_2}$: Δ decayed pion 3-d momentum in the frame of Δ at rest

$\boldsymbol{J_0(\beta q_r)}$:

0th-order Bessel function

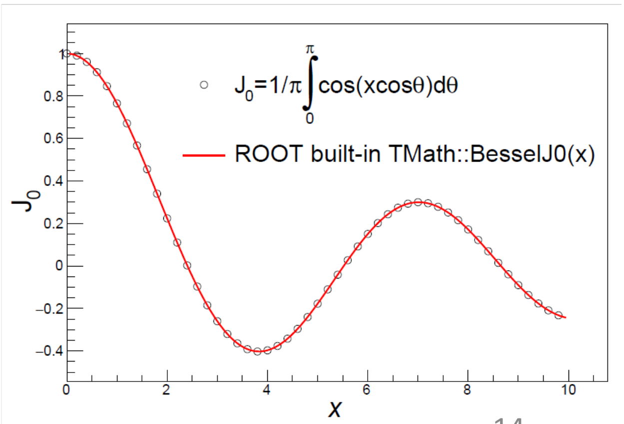

[1] H. Shimizu, ELPH Annual Report, 2017; **[2]** Q. He, in *J. Phys. Conf. Ser. 1643*, 012010 (2020).

Correlation observation model

Correlation functions at different p_2

$$C_{BEC}(q,p_2) = 1 + \lambda \exp(-\alpha^2 q_z^2) \exp\left(-\frac{\alpha^2 q_r^2}{2}\right) J_0\left(\frac{q_r}{2p_2}\right)$$

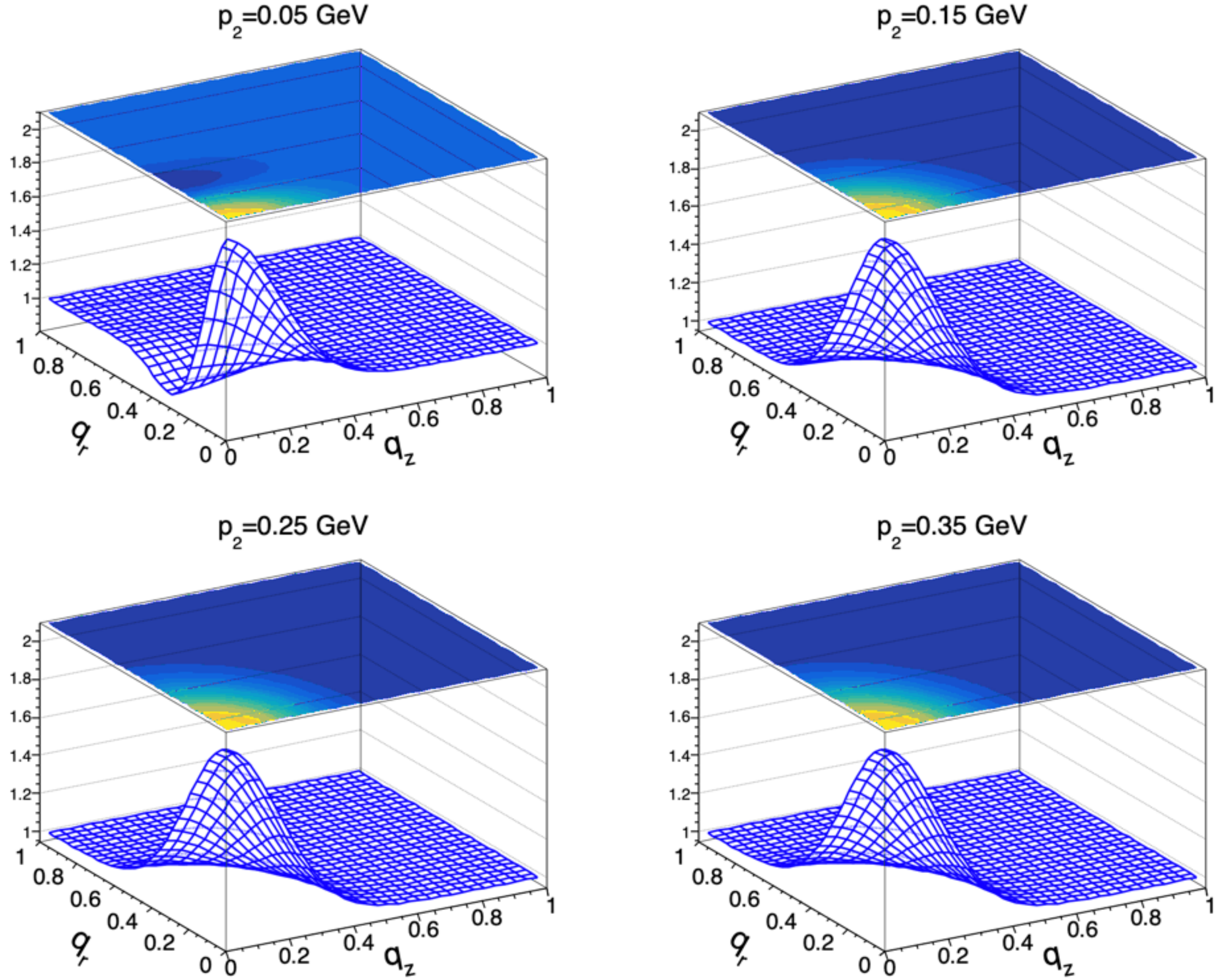

Results of FOREST and BGOegg experiments

FOREST Experiment

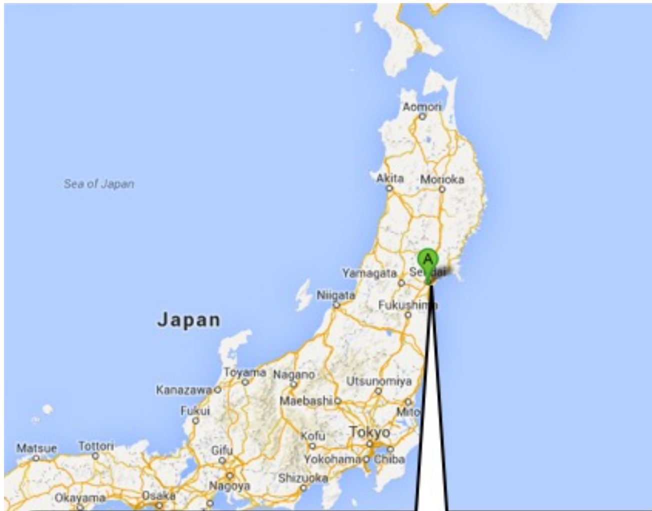

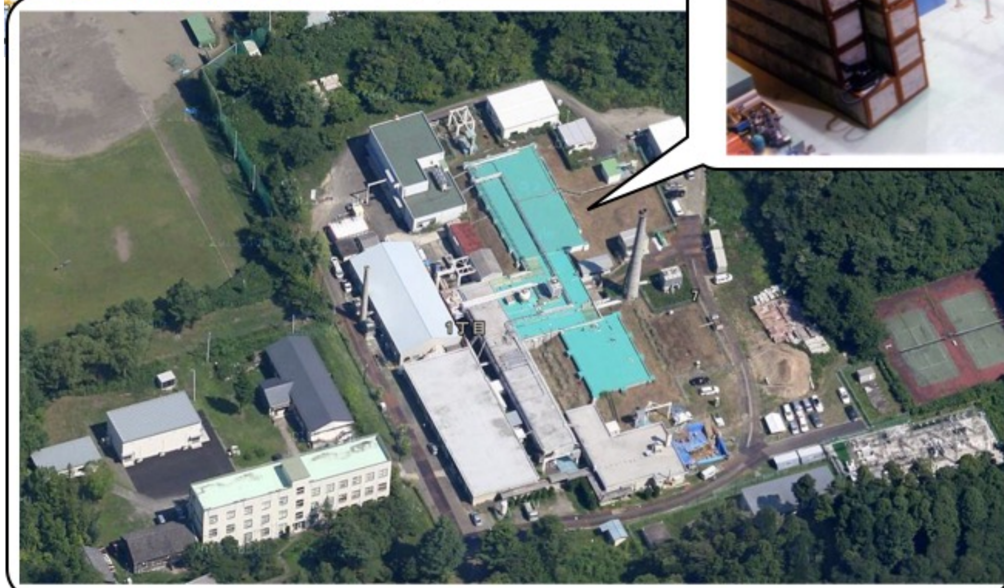

0.5-1.2 GeV photon beam

$$\gamma p \rightarrow \pi^0 \pi^0 p$$

Results of FOREST and BGOegg experiments

4π Electromagnetic detector complex FOREST

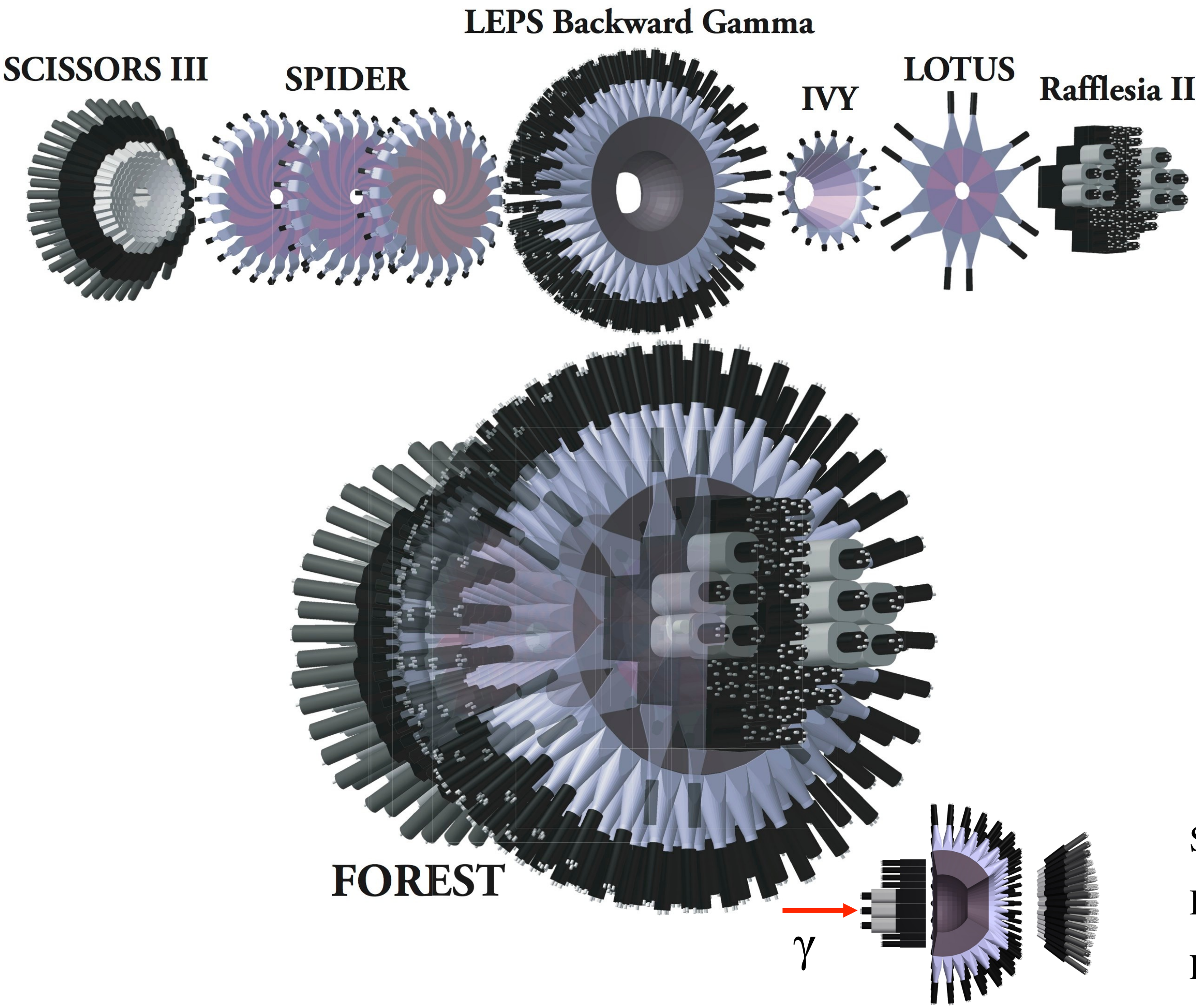

EM Calorimeter

SCISSORS III
192 CsI; θ: 4°-24°, φ:full
Res. : 3% @ 1GeV

Backward Gamma
252 Lead/Scintillating fiber modules;
θ: 30°-100°, φ:full
Res. : 7% @ 1GeV

Rafflesia II
62 Lead Glass modules;
Res. : 5% @ 1GeV

Plastic Scintillator

SPIDER (2 layers × 24 modules

IVY (18 modules)

LOTUS (12 modules)

Results of FOREST and BGOegg experiments

Identification of $\gamma p \to \pi^0\pi^0 p$

π^0

$\pi^0 \to 2\gamma$

- Two **neutral clusters** with Δt=[-1.5,1.5] ns.
- Invariant mass = $M_{\pi 0}$

$m^2_{\gamma\gamma} = 2E_{\gamma 1}E_{\gamma 2}(1-\cos\theta_{\gamma 1\gamma 2})$

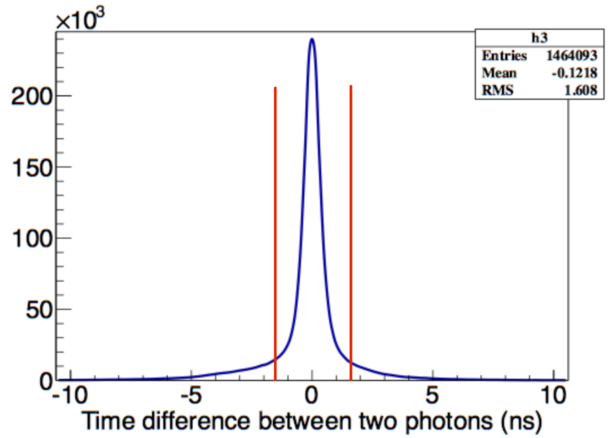

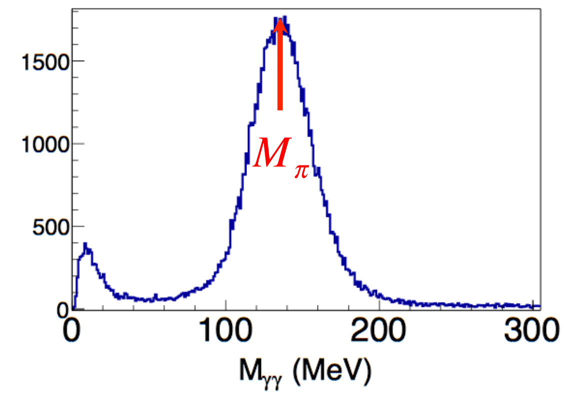

Proton

- Delayed **charged cluster** wrt. the average time of the selected 2 pairs of coincident photons (**$t_{4\gamma}$**)
- Miss mass Mx of $\gamma p \to \pi^0\pi^0 X$ is equal to the proton mass

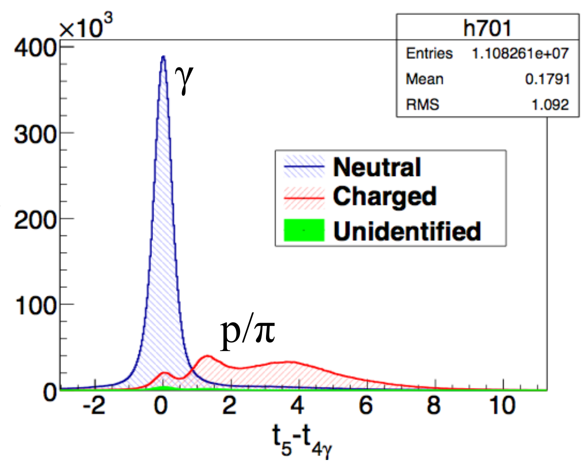

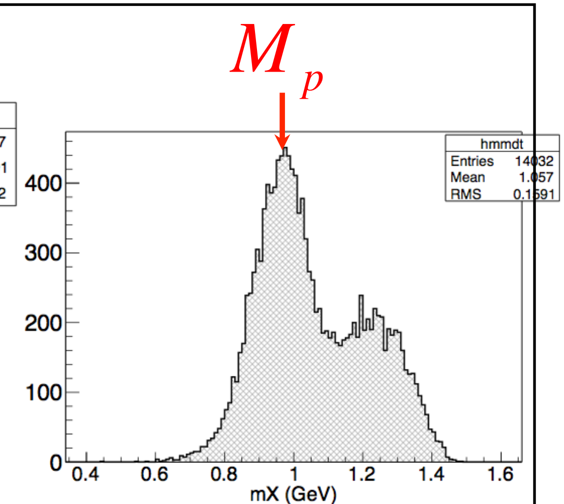

Results of FOREST and BGOegg experiments

Invariant mass and missing mass

The best combinations of the two paris of photons

Missing mass distribution of the hypothesis $\gamma p \rightarrow \pi^0 \pi^0 X$

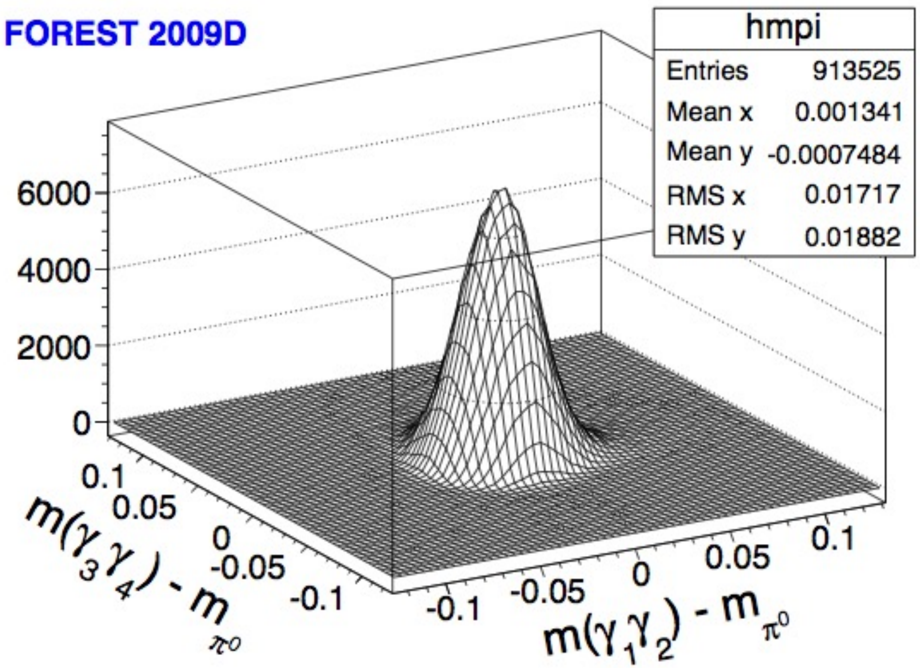

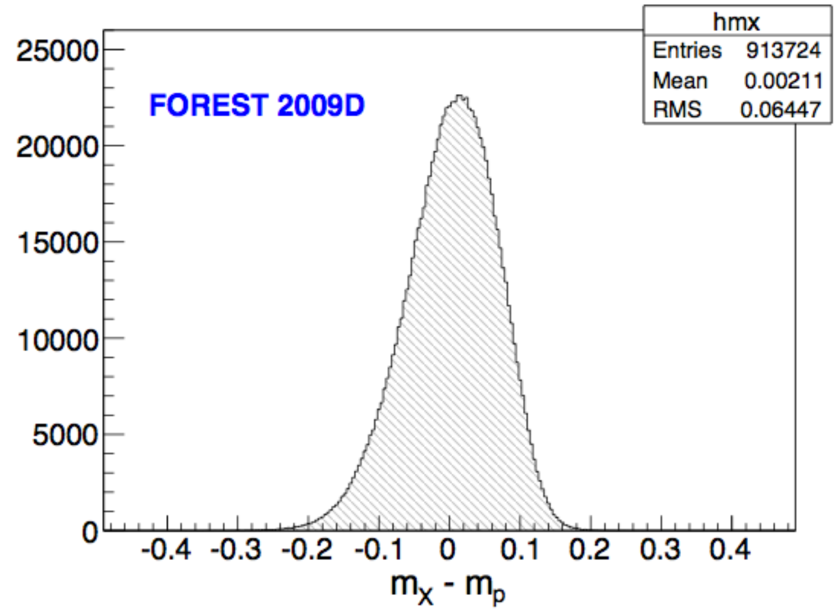

Results of FOREST and BGOegg experiments

$\gamma p \to \pi^0 \Delta \to \pi^0 \pi^0 p$ process is dominant in $\gamma p \to \pi^0 \pi^0 p$

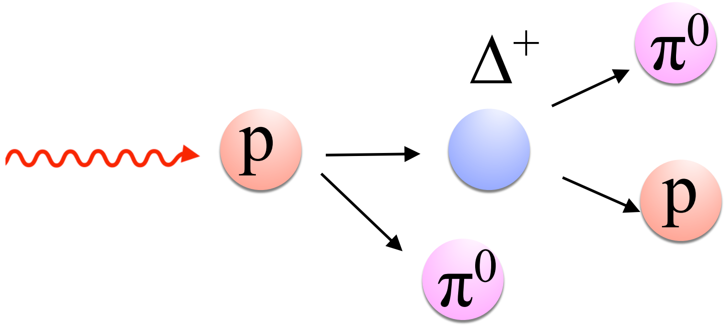

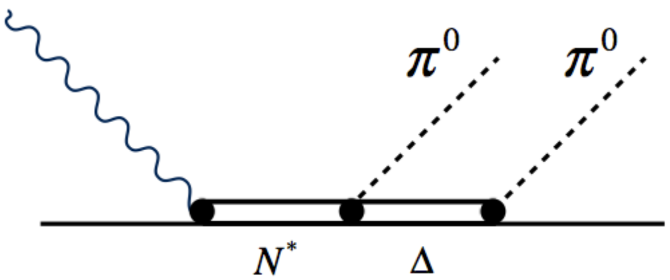

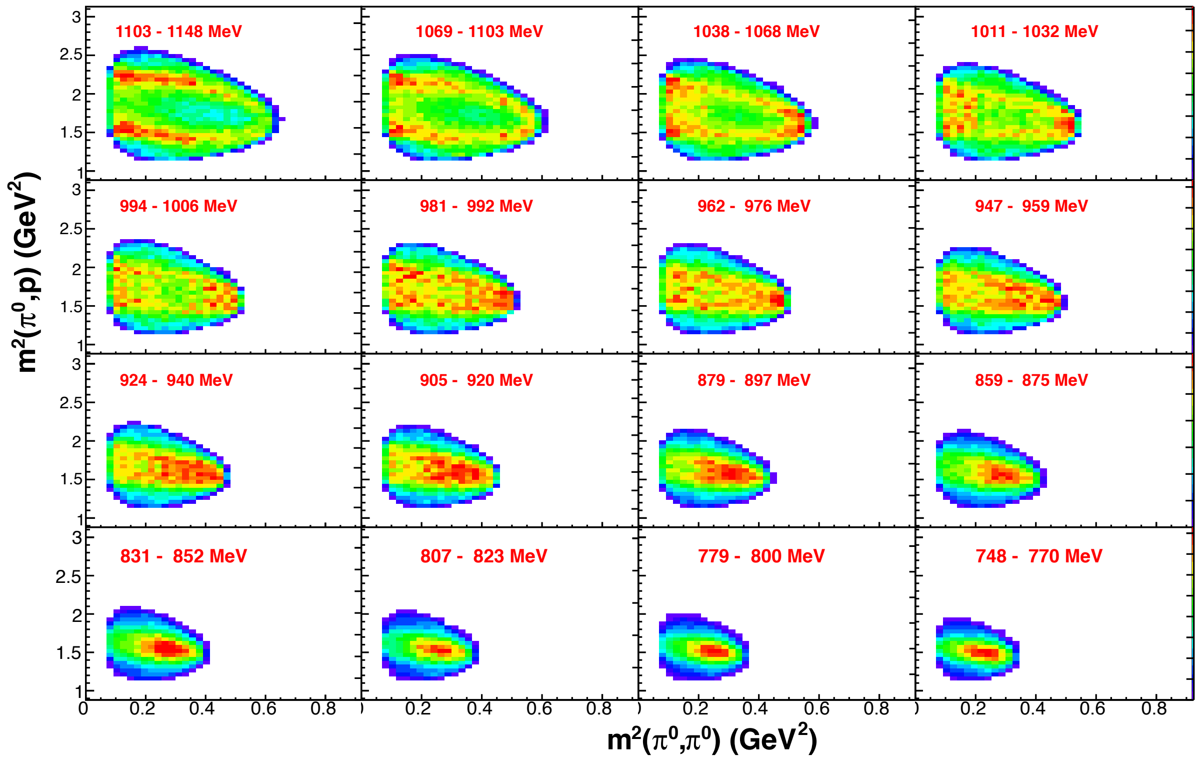

[1] Q. He, in *J. Phys. Conf. Ser. 1643*, 012010 (2020)

Results of FOREST and BGOegg experiments

$\pi^0\pi^0$ correlations

Correlation function:

Signal sample: $\pi^0\pi^0$ relative momentum distribution

$$g^{(2)}(p_1, p_2) = \frac{I_{12}(p_1, p_2)}{I_1(p_1)I_2(p_2)}$$

Reference sample : $\pi^0\pi^0$ relative momentum distribution

Assuming Gaussian density distribution of emitting source

$$g^{(2)}(Q) = N(1 + \lambda_2 e^{-r_0^2 Q^2})$$

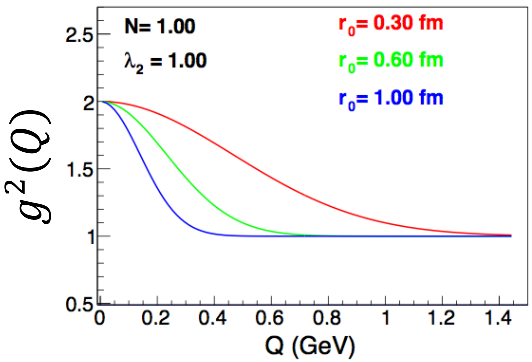

$$Q^2 = -(p_1 - p_2)^2 = (p_1 + p_2)^2 - 4\mu^2$$

Constructed by event mixing method, in which a reference event is built by taking two π^0s from different events.

Appropriate mixing cut is required!

A package named ‘**EMBEC**’ based on **ROOT** framework prepared to perform event mixing

Results of FOREST and BGOegg experiments

Preliminary results of $\pi^0\pi^0$ correlations in $\gamma p \rightarrow p\pi^0\pi^0$

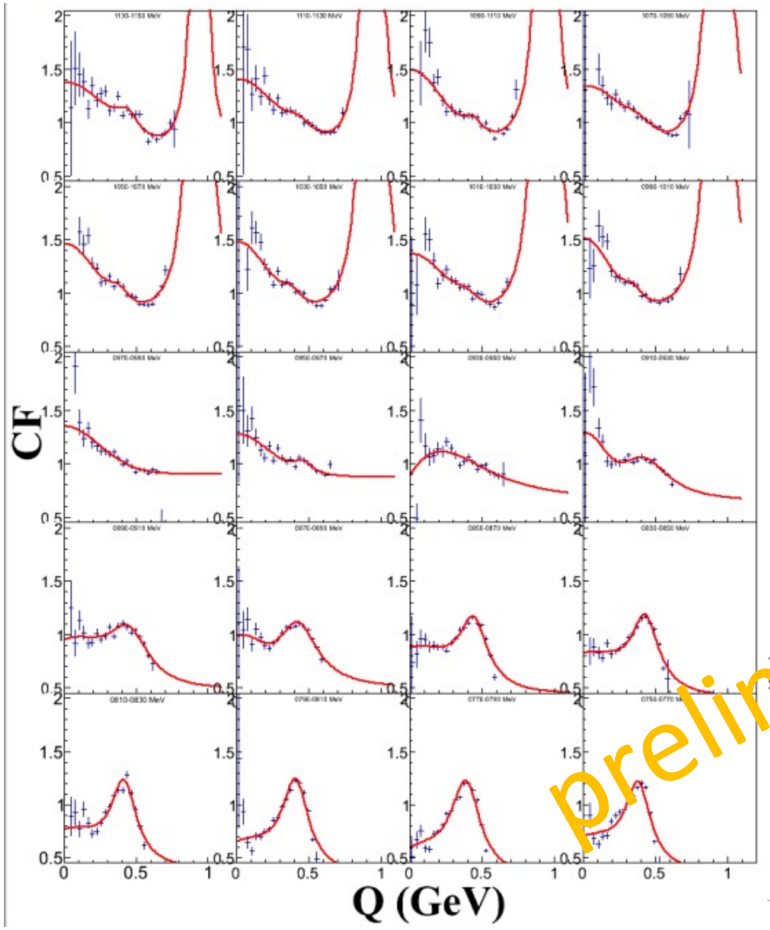

Fitting trial (4)

$$fit(Q) = N_1\left(1 + \lambda_2 EXP(-r_0^2 Q^2)\right) + N_2 \frac{M_\sigma^2 \Gamma_\sigma^2}{\left(Q^2+4m_\pi^2-M_\sigma^2\right)^2 + M_\sigma^2\Gamma_\sigma^2} \frac{Q}{8\pi\sqrt{Q^2+4m_\pi^2}} + N_3 \frac{M_{f980}^2 \Gamma_f^2}{\left(Q^2+4m_\pi^2-M_{f980}^2\right)^2 + M_{f980}^2\Gamma_f^2} \frac{Q}{8\pi\sqrt{Q^2+4m_\pi^2}}$$

Fixed parameters:

$M_{f980} = 980\ MeV$

Limited parameters:

λ_2=[0,1]

$M_\sigma = [300,700]\ MeV$

$\Gamma_\sigma = [100,700]\ MeV$

Fit results:

radius

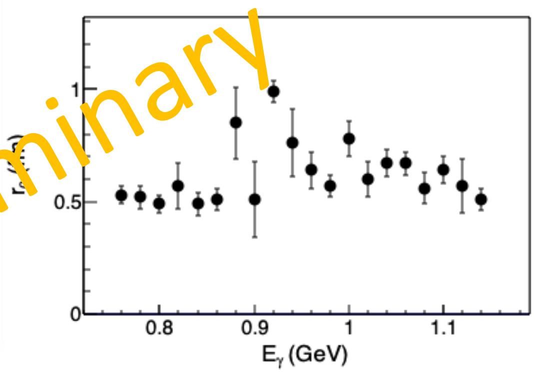

lambda

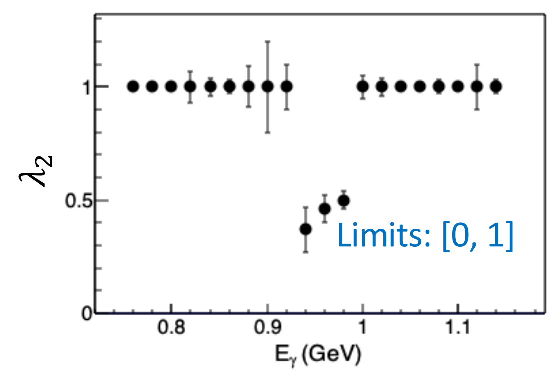

Results of FOREST and BGOegg experiments

LEPS2/BGOegg Experiment @ Spring-8

LEPS2/BGOegg Experiments

A large acceptance electromagnetic (EM) calorimeter BGOegg (Fig.1) was constructed at ELPH, Tohoku University. This calorimeter system has been transferred to the new laser Compton scattering beamline LEPS2 at SPring-8, where a 1.3-2.9 GeV photon beam with high linear polarization is available. The phase-1 experiments have started from 2014 April with the EM calorimeter BGOegg and the additional detectors for charged particles. We are now upgrading the experimental setup by covering most of the solid angles with EM calorimeters to start new data collection in the phase-2 experiments.

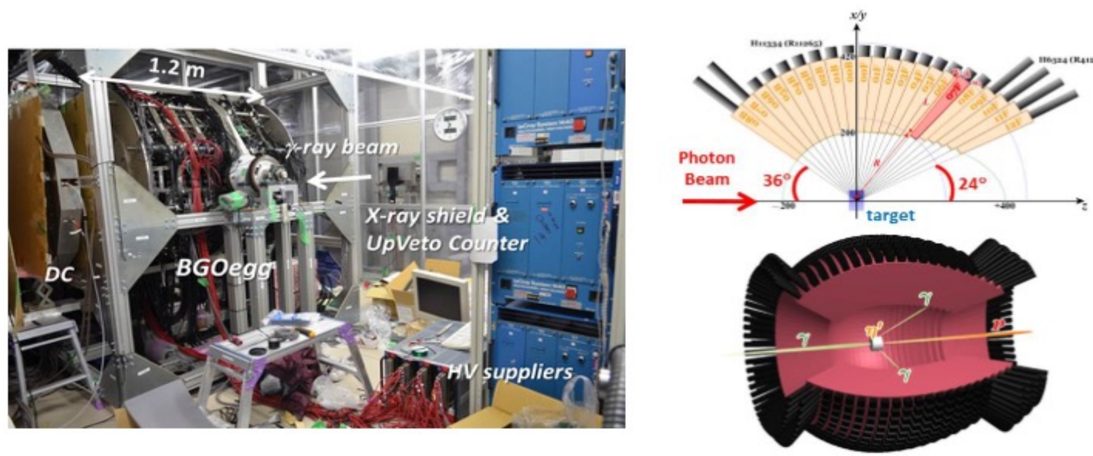

Fig.1 A picture of BGOegg inside the thermostatic booth (Left) and the drawings of BGOegg (Right).

Physics

Results of FOREST and BGOegg experiments

LEPS2/BGOegg Experiment @ Spring-8

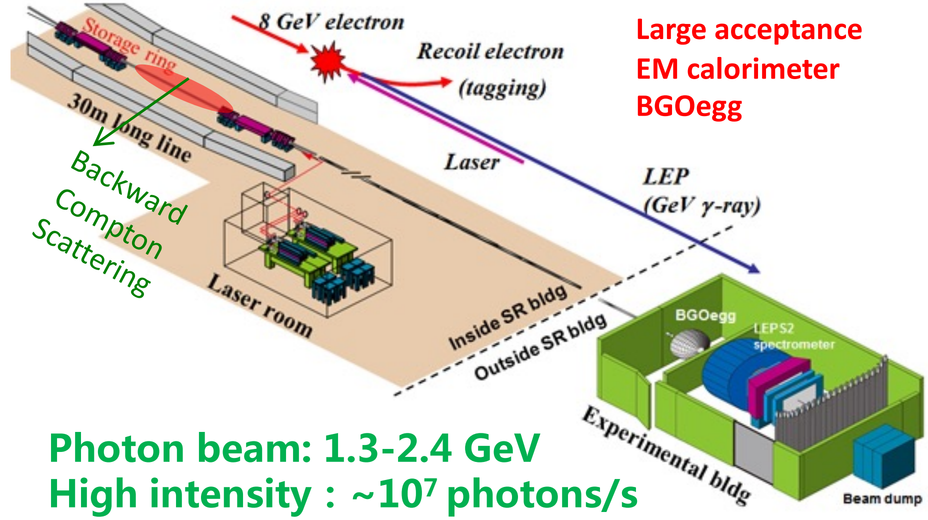

Large acceptance
EM calorimeter
BGOegg

Photon beam: 1.3-2.4 GeV
High intensity : ~10^7 photons/s

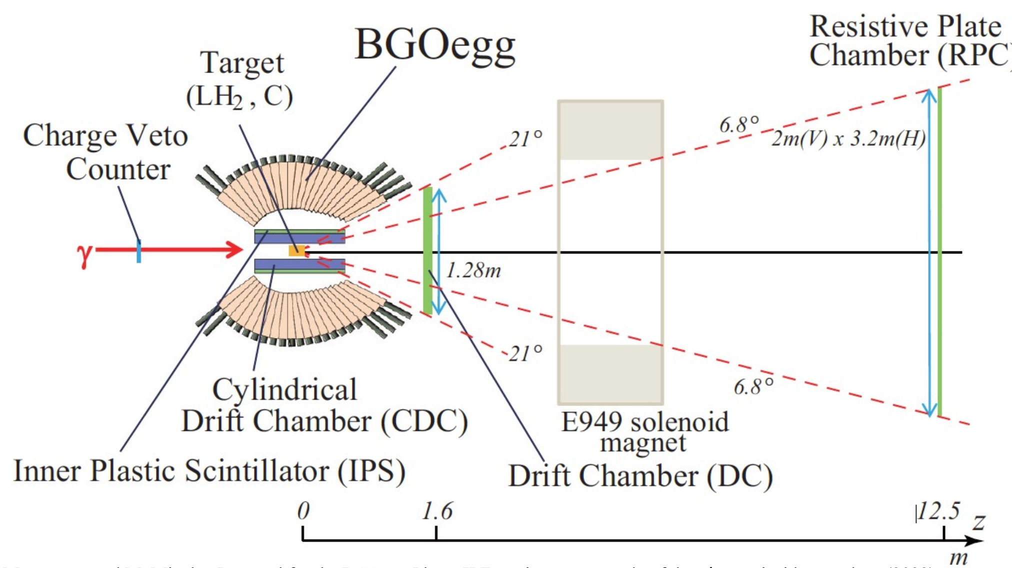

1. N. Muramatsu and M. Miyabe, Proposal for the BGOegg Phase-II Experiment – A study of the η' mass inside a nucleus (2022)
2. H. Shimizu, A trial to measure a spectral function of η' mesons, ELPH Annual Report 2017, 103 (2017)
3. Yuji Matsumura, Calibration and performance of the BGOegg calorimeter, ELPH Workshop, C010, (2015)

Results of FOREST and BGOegg experiments

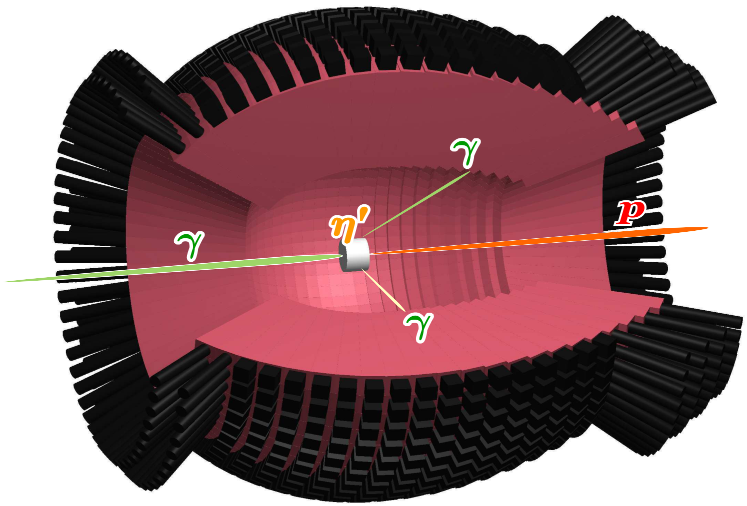

EM calorimeter BGOegg

- 1320 BGO crystals (22 layers × 60)
- coverage : 24°-156° in polar angle
- Crystal length: 220 mm长 (~20X_0) ，

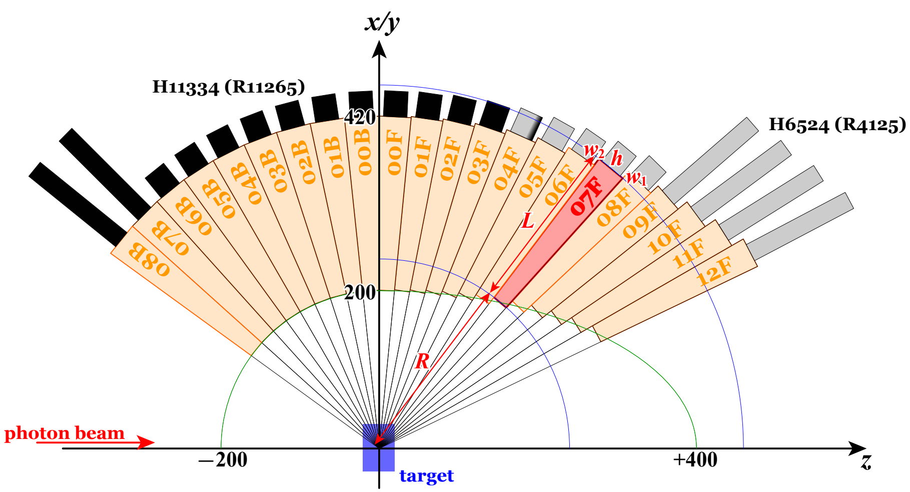

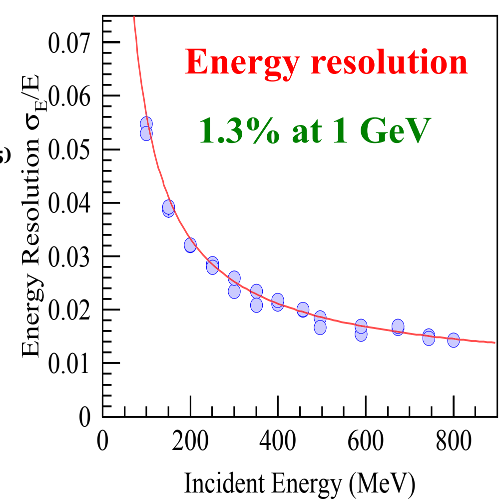

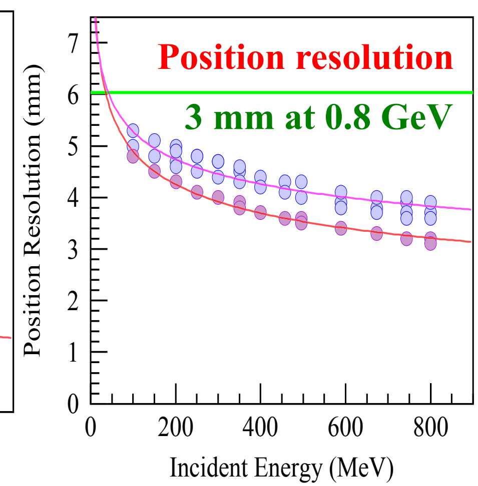

Results of FOREST and BGOegg experiments

Forward drift chamber

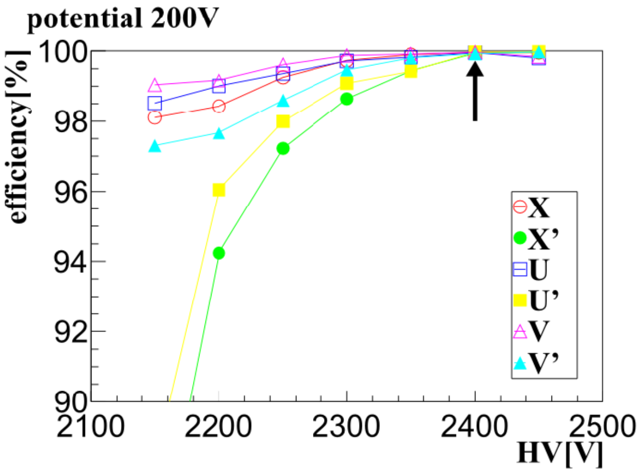

w.r.t the vertical plane

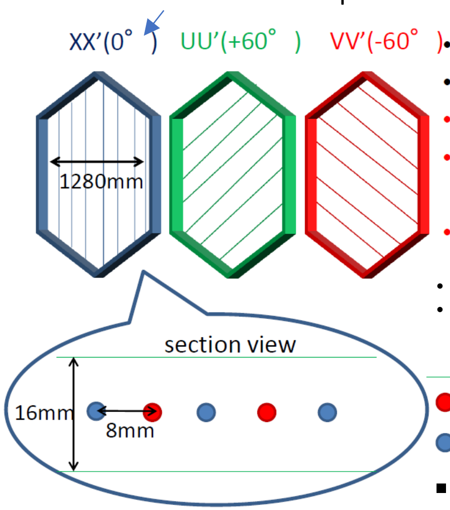

- hexagonal frame
- Diameter of incircle is 1280 mm
- 16 mm square cell
- 6 layer
  -XX'(0°),UU'(+60°),VV'(-60°)
- 80 ch/layer

- **Ar/C4H10 gas (but P10 gas in Dec. runs)**
- **Drift times is recorded by LeCroy TDC 3377**

Cathode (Alminized Mylar) 25 μm
Sense wire(Au-W) Φ30 μm
Potential wire(Au-BeCU) Φ80μm

- 480 readout channels
- Coverage: 0°-22° (polar angle)
- No magnetic field

Position resolution

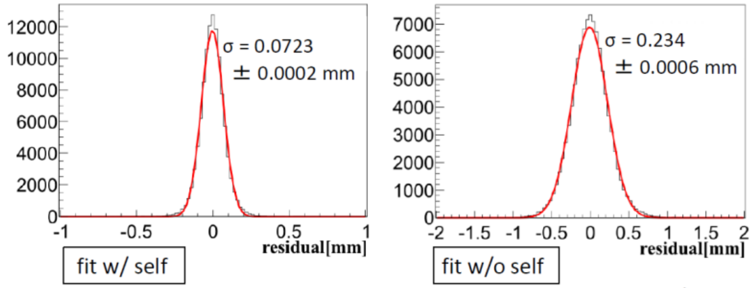

σ_1 : residual's σ by fit w/ self

σ_2 : residual's σ by fit w/o self

$$\sigma_{intrinsic} = \sqrt{\sigma_1 \cdot \sigma_2}$$

$\sigma_{intrinsic}$ = 130 ± 0.2 μm

Ref.: N. Muramtsu, LEPS2/BGOegg experiment, Q-PAC, 2014,1.29

Results of FOREST and BGOegg experiments

Event selection of $\gamma p \to \pi^0\pi^0 p$

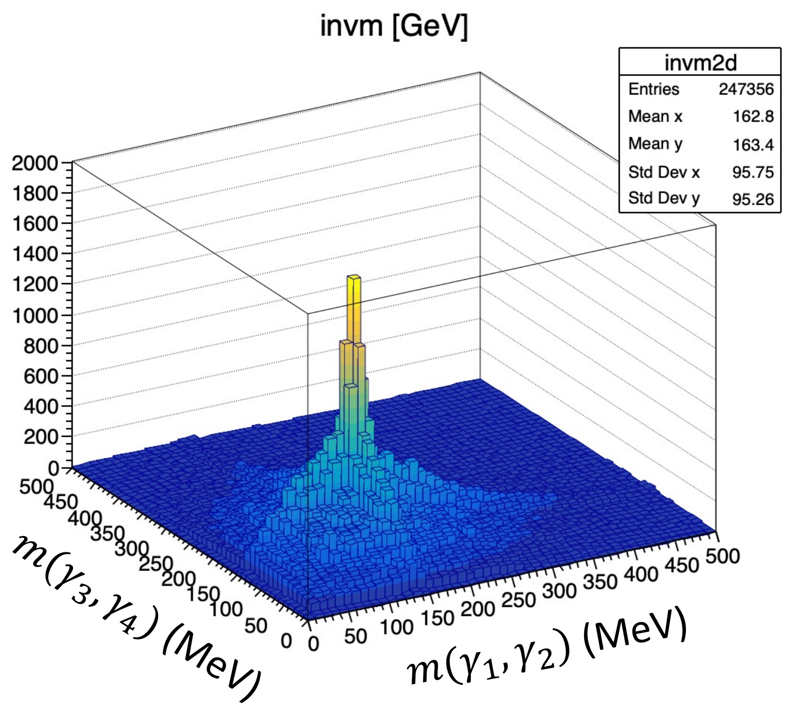

Kinematic fitting

$$L(\eta,\xi,\lambda) = (\eta - y)^T C_y^{-1} (\eta - y) + \lambda^T f(\eta,\xi) = minimum$$

Dataset: 2014B

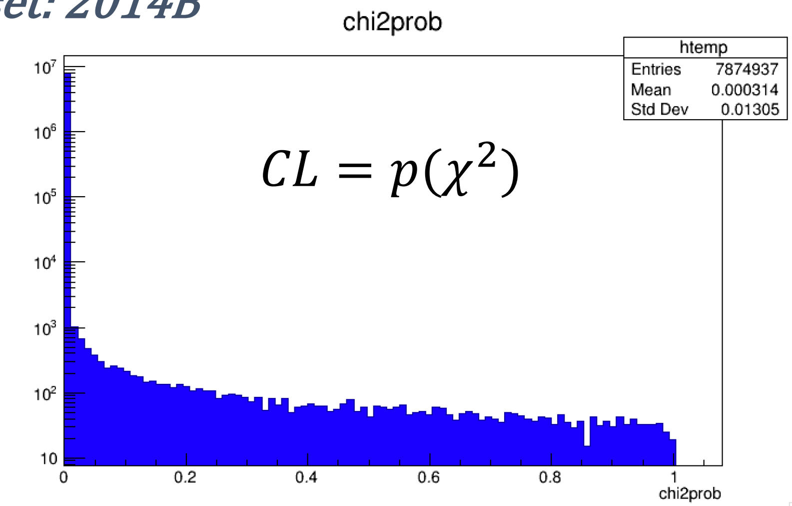

$PULL(E_1)$

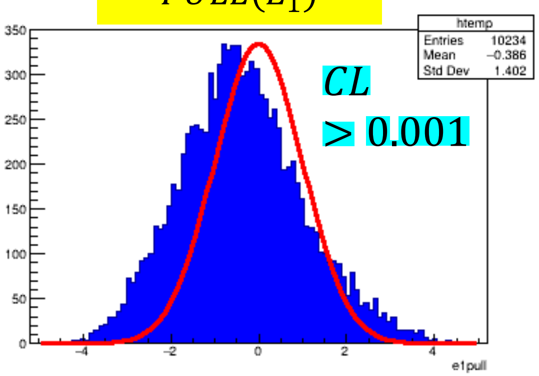

$PULL(\theta_1)$ $(CL > 0.001)$

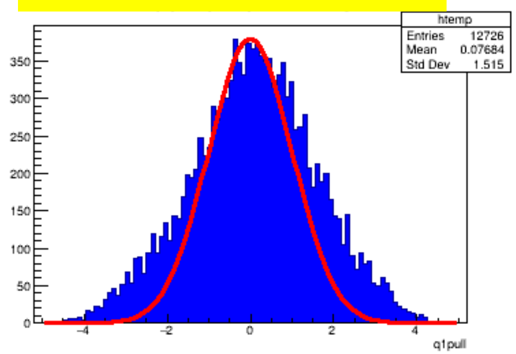

$PULL(\phi_1)$ $(CL > 0.001)$

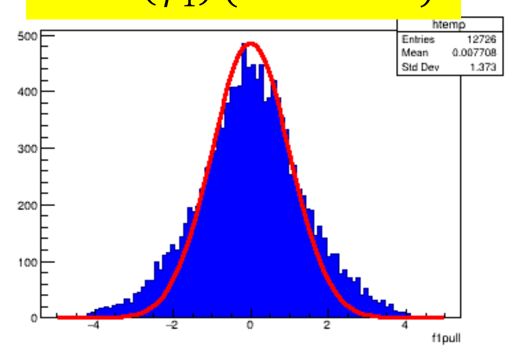

Data

Gaus.(0,1)

Results of FOREST and BGOegg experiments

$\pi^0\pi^0$ Correlation functions

$$g^{(2)}(p_1, p_2) = \frac{I_{12}(p_1, p_2)}{I_1(p_1) I_2(p_2)}$$

$$g^{(2)}(Q) = N(1 + \lambda_2 e^{-r_0^2 Q^2})$$

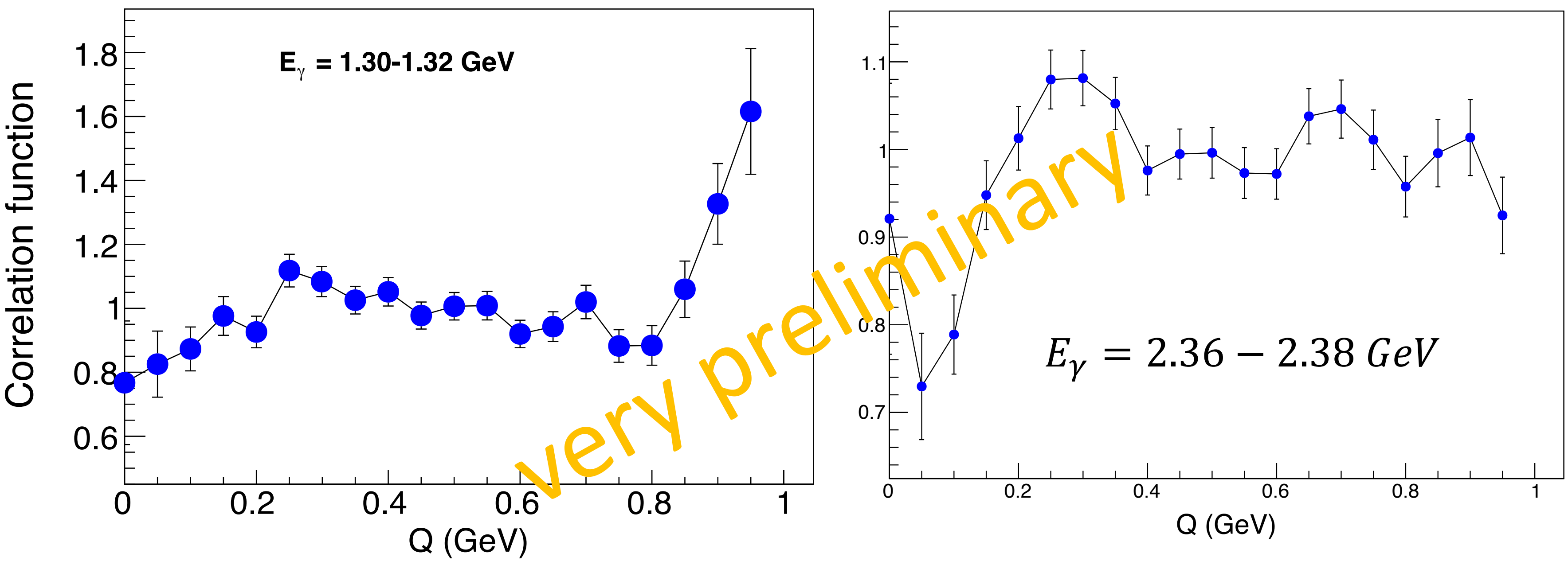

Summary

- Preliminary BEC results on FOREST experiments get the Gaussian radius of the intermediate state ($\Delta(1232)$ resonance is dominant) in $\gamma p \rightarrow \pi^0\pi^0 p$ around $E_\gamma \sim 1\ GeV$

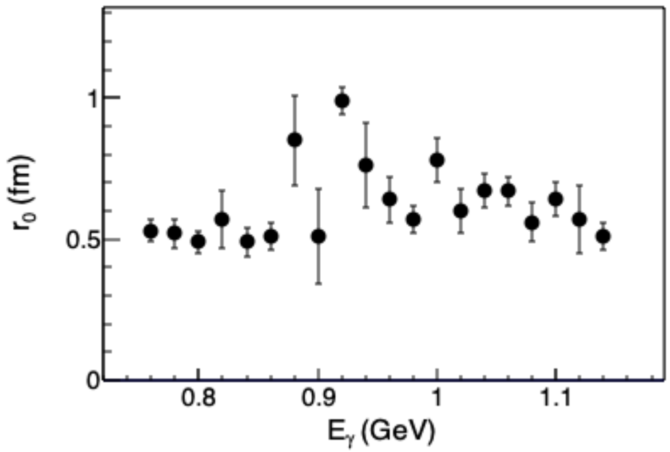

- Still need to refine this analysis to get BEC results from pure $\Delta(1232)$ events and to estimate the systematic errors…

- A very preliminary $\pi^0\pi^0$ correlation results with EMBEC analysis method for BGOegg experimental data in the photon beam energy region (1.3-2.4 GeV) are obtained. More accurate results are on the way.

Other physics studies at BGOegg

- ❑ η′ mass inside a nucleus
- ❑ f_1(1285) meson photoproduction
- ❑ Photoproduction of η′ mesons from nuclei near the production threshold
- ❑ Photon beam asymmetry of the η′ photoproduction on the proton

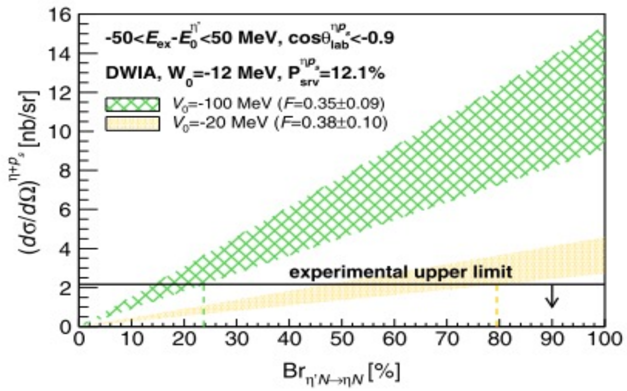

FIG. 4. The experimental upper limit of $(d\sigma/d\Omega)^{\eta+p_s}_{\rm exp}$ at the 90% confidence level, and $(d\sigma/d\Omega)^{\eta+p_s}_{\rm theory}$ as a function of $\mathrm{Br}_{\eta' N\to\eta N}$.

Phys. Rev. Lett. **124**, 202501 (2020).

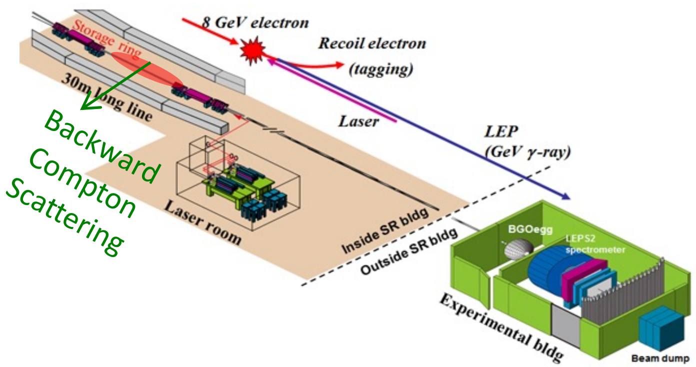

Thanks for your attention